Alexander A. ALEXANDRIDIS*, Janusz P. GOLDASZ**

SIMPLIFIED MODEL OF THE DYNAMICS OF MAGNETO-RHEOLOGICAL DAMPERS

SUMMARY

It has been long recognized that the inertia and compressibility of the fluid have a significant effect on the dynamic behavior of Magneto-Rheological (MR) dampers. Previous studies have revealed the nature of the effect through the analysis of a comprehensive, albeit fairly complex, state-space model of the MR monotube damper hydraulics. The present paper outlines a simpler model of the damper and presents simple analytical expressions for the transfer function between the input velocity (or stroke) and the output force. Pistons with single and dual flow passages are analyzed. In addition, simple expressions for the damper natural frequency and damping ratio are given. Finally, the transfer functions are presented analytically as well as in the form of Bode plots of the amplitude and the phase angle of the transfer functions vs. the normalized frequency.

Keywords*: magnetorheological damper, fluid compressibility, fluid inertia, damper dynamics*

UPROSZCZONY MODEL DYNAMIKI TŁUMIKA MAGNETOREOLOGICZNEGO

Od dawna wiadomo, że bezwładność i ściśliwość cieczy ma znaczący wpływ na właściwości dynamiczne tłumików magnetoreologicznych (MR). W poprzednich badaniach prezentowano model w przestrzeni stanu, powstały w wyniku szczegółowej analizy, aczkolwiek stosunkowo skomplikowanej, opisujący właściwości hydraulicznego tłumika MR z pojedynczym cylindrem. Niniejszy artykuł prezentuje uproszczony model tłumika wraz z prostymi zależnościami określającymi funkcję przejścia pomiędzy wejściem w postaci prędkości (przemieszczenia) a wyjściem w postaci siły. Analizowano układy z tłokiem z pojedynczą oraz podwójną szczeliną przepływową. Ponadto zamieszczono proste wyrażenia na częstotliwość drgań własnych tłumika oraz współczynnik tłumienia. Na zakończenie zaprezentowano funkcje przejścia w postaci analitycznej oraz wykresów Bodego.

1. INTRODUCTION

Investigation of the dynamic behavior of Magneto-Rheological (MR) dampers subjected to a short-stroke, medium- or high-frequency excitation has revealed unusual characteristics best described as a clockwise rotation of the damping force vs. displacement characteristic curves ("ellipses") with increasing stroking frequency. The same phenomenon is responsible for the hysteretic behavior seen in the force vs. piston velocity characteristics. Figures 1–4 illustrate the (simulated) behavior of MR dampers with and without current applied. In Reference [1] the authors made the hypothesis that the most likely causes are the fluid *inertia* and *compressibility* (bulk modulus) and carried out an analysis of the fairly detailed MR damper model of Figure 5 in order to quantify the effects of the fluid properties on the dynamics of the MR dampers. The model described in [1] accounts for the compressibility of the fluid chambers, laminar losses through the piston annular flow path(s), and the inertia of the fluid element occupying the annulus (the "slug"). The

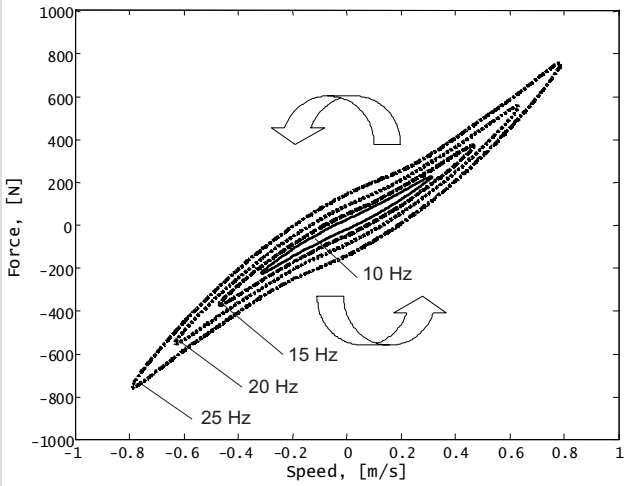

Fig. 1. Off-state (zero current) force-velocity phase plane

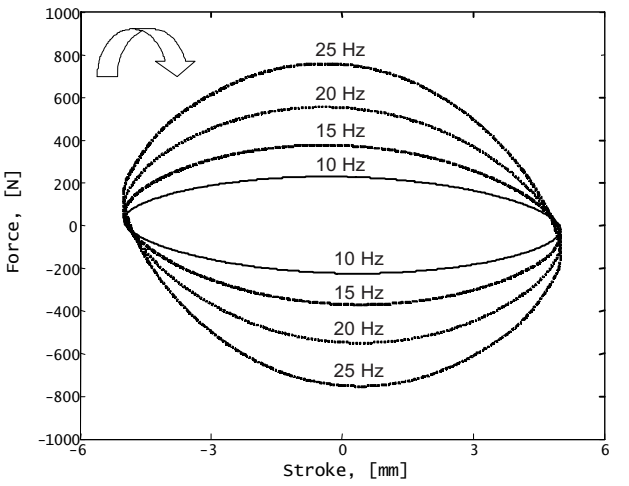

Fig. 2. Off state force-displacement phase plane

* Delphi Corporation, Brighton Technical Center, Brighton, Michigan, USA
** Delphi Corporation, Kraków Technical Center, Cracow Poland

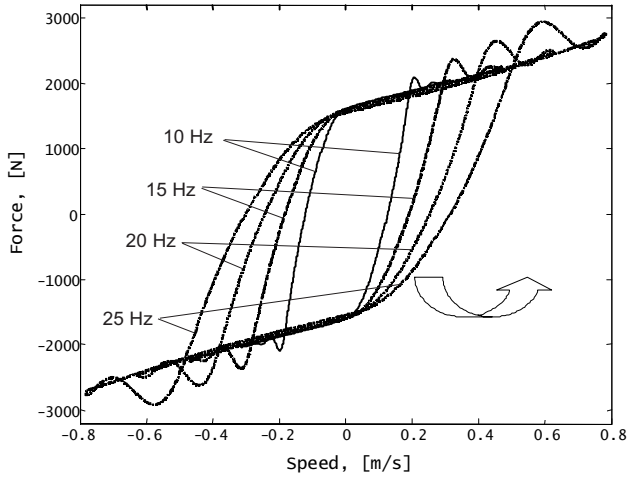

Fig. 3. On-state (current applied) force-velocity phase plane

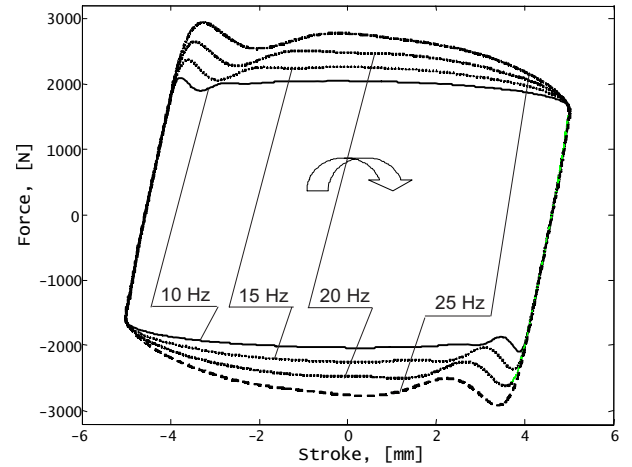

Fig. 4. On-state force-displacement phase plane

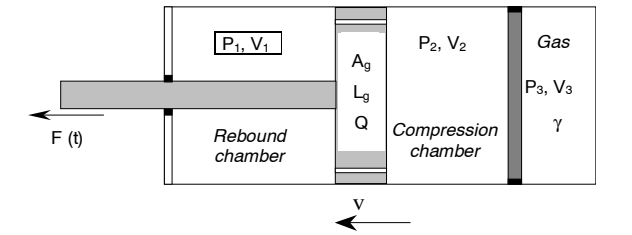

Fig. 5. Monotube MR damper configuration [1]

piston and rod assembly (P&R) dynamics were taken into account as well. The numerical calculations carried out in [1] identified two vibration modes. The primary one relates to the fluid element dynamics, whereas the second (higher) resonant frequency is due to the combined inertia of the P&R and the fluid element.

The present study is motivated by the observation that the P&R inertia has little or no effect under normal working conditions (stroking frequencies up to approximately 50 Hz) and can be eliminated leading to a reduced-order, stroke-driven system. The (original) force-driven system and the (simpler) reduced-order one can then be analyzed and compared in terms of the first natural frequency, Ω_F. Therefore, in Section 2 the authors derive the simplified model input-output relationships and define the system transfer function. Section 3 shows an approach towards generalizing the results and expressing them in terms of the parameters of a mechanically analogous mass-spring-damper system. Moreover, an extension of the method for MR dampers having two or more annular flow paths in the piston is outlined in Section 4. Section 5 contains configuration-specific damper data. The analytical results are presented in Section 6 and the conclusions are drawn in Section 7.

2. DAMPER MODEL WITH PRESCRIBED STROKING VELOCITY

In this section a damper model that is driven by a prescribed piston motion is developed. A starting point for the analysis is the model described and analyzed in [1], which can be reduced by eliminating the inertia of the P&R assembly from the system dynamics. Thus, the original fourth-order system is reduced to a second-order system driven by the (prescribed) stroking velocity input (as opposed to force-driven). The stroke-driven model layout is shown in Figure 6. For this configuration the dynamics at mid-stroke can be derived as follows:

$$\frac{dP_1}{dt} = \frac{\beta}{V_0}\left[-Q + A_p v\right]$$

$$\frac{dP_2}{dt} = \frac{\beta}{V_0}\left[Q - A_p v\right] \tag{1}$$

$$\frac{dQ}{dt} = \frac{A}{\rho L}\left[P_1 - P_2 - RQ\right]$$

where P_1, P_2 are the upper and lower chamber pressures. Q denotes the flow rate through the piston flow path, whereas β and ρ refer to the fluid bulk modulus and density, respectively. R represents the (laminar) hydraulic resistance of the flow path. Finally, V_0 is the fluid volume (per chamber) at mid-stroke. Hence, the state-space representation takes the following form

$$\frac{dX}{dt} = AX + Bv \tag{2}$$

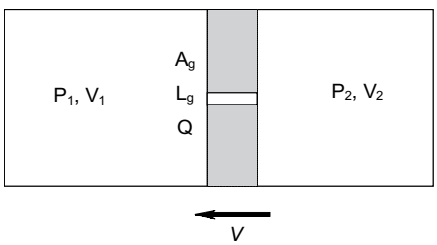

Fig. 6. Reduced (stroke velocity-driven) symmetric actuator configuration

where $X = [P_1 \quad P_2 \quad Q]^T$

$$A = \begin{vmatrix} 0 & 0 & -\beta\frac{1}{V_0} \\ 0 & 0 & \beta\frac{1}{V_0} \\ \frac{A_g}{\rho L_g} & -\frac{A_g}{\rho L_g} & -R_h\frac{A_g}{\rho L_g} \end{vmatrix}$$

$$B = \begin{vmatrix} 0 & 0 & \beta\frac{A_p}{V_0} \\ 0 & 0 & -\beta\frac{A_p}{V_0} \\ 0 & 0 & 0 \end{vmatrix}$$

Then, the output is the damping force F, given by

$$F = (p_1 - p_2)A_p \tag{3}$$

As a result, the transfer function between the force and the input velocity is

$$H_v(s) = \frac{F(s)}{V(s)} = \frac{2\beta\frac{A_p^2}{V_0}\left(s + \frac{A_g}{\rho L_g}R_h\right)}{s^2 + s\frac{A_g}{\rho L_g}R_h + 2\frac{A_g}{\rho L_g}\frac{\beta}{V_0}} \tag{4}$$

The natural frequency is given by

$$\Omega_F = \sqrt{\frac{2\beta}{V_0}\frac{A_g}{\rho L_g}} \tag{5}$$

3. MECHANICAL SINGLE-DEGREE-OF-FREEDOM ANALOGY

This Section outlines an approach towards casting the transfer function of Equation (4) in terms of the parameters of an equivalent, mechanically analogous (mass-spring-damper) system. Let:

$$\begin{aligned} m_g &= \rho A_g L_g & c_0 &= R_h A_g^2 \\ k_g &= \beta\frac{A_g^2}{V_g} & c_{cr,g} &= 2\sqrt{k_g m_g} \\ \omega_g^2 &= \frac{k_g}{m_g} & \zeta_g &= \frac{c_0}{c_{cr,g}}\sqrt{\frac{V_0}{2V_g}} \\ \Omega_F^2 &= \omega_g^2 2\frac{V_g}{V_0} & \mathrm{B} &= \frac{\omega}{\Omega_F} \end{aligned} \tag{6}$$

Then, Equation (4) becomes

$$H(s) = \frac{F(s)}{V(s)} = \frac{2k_0\left(s + 2\zeta_g\Omega_F\right)}{s^2 + 2\Omega_F\zeta_g s + \Omega_F^2} \tag{7}$$

Therefore, the Amplitude Ratio is given by

$$\left|H_v(\mathrm{B})\right|\frac{\Omega_F}{2k_0} = \sqrt{\frac{\mathrm{B}^2 + \left(2\zeta_g\right)^2}{\left(1-\mathrm{B}^2\right)^2 + \left(2\zeta_g\mathrm{B}\right)^2}} \tag{8}$$

The Phase Angle is given by

$$\phi(\mathrm{B}) = \arctan\frac{\mathrm{B}}{2\zeta_g}\left(1 - \mathrm{B}^2 - 4\zeta_g^2\right) \tag{9}$$

4. DUAL-PATH PISTON DYNAMICS

The dual-path piston shown in Figure 7 is described in detail in the US Patent 6,279,701 [2].

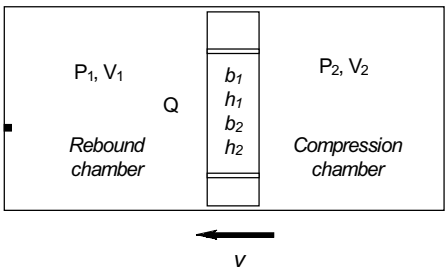

Fig. 7. Dual-path piston layout: linear model

Briefly, the piston features two (or more) parallel flow paths and offers the advantages of digressive force vs. velocity characteristics, shorter piston length, and a higher turn-up ratio. The equations of motion in the state-space format are:

$$\begin{aligned} \frac{dP_1}{dt} &= \frac{\beta}{V_0}\left[-Q + A_p v\right] \\ \frac{dP_2}{dt} &= \frac{\beta}{V_0}\left[Q - A_p v\right] \\ \frac{dQ_1}{dt} &= \frac{A_1}{\rho L_1}\left[P_1 - P_2 - R_1 Q_1\right] \\ \frac{dQ_2}{dt} &= \frac{A_2}{\rho L_2}\left[P_1 - P_2 - R_2 Q_2\right] \\ Q &= Q_1 + Q_2 \end{aligned} \tag{10}$$

where Q_1, Q_2 are the volume flow rates through the two flow paths of the piston. The above system of equations describes the pressure variation in each pressure chamber and the dynamics of the two fluid elements occupying the two flow paths. Re-arranging the above equations into the state-space format provides the following transfer function for the dual-path piston model

$$H_v(s)=2\frac{\beta}{V_0}A_p^2\frac{s^2+s\left(R_1\frac{A_1}{\rho L_1}+R_2\frac{A_2}{\rho L_2}\right)+R_1\frac{A_1}{\rho L_1}R_2\frac{A_2}{\rho L_2}}{s^3+s^2\left(R_1\frac{A_1}{\rho L_1}+R_2\frac{A_2}{\rho L_2}\right)+s\left[R_1\frac{A_1}{\rho L_1}R_2\frac{A_2}{\rho L_2}+2\frac{\beta}{V_0}\left(\frac{A_1}{\rho L_1}+\frac{A_2}{\rho L_2}\right)\right]+2\frac{\beta}{V_0}\frac{A_1}{\rho L_1}\frac{A_2}{\rho L_2}(R_1+R_2)} \tag{11}$$

The above transfer function can also be cast in terms of a mechanically analogous system.
Let:

$$k_0=\frac{\beta}{V_0}A_p^2 \qquad k_i=\frac{\beta}{V_i}A_i^2 \qquad m_i=\rho A_i L_i$$

$$\zeta_i=\frac{R_i A_i^2}{2\sqrt{k_i m_i}\sqrt{\frac{V_i}{2V_0}}} \quad \Omega_i^2=2\frac{\beta}{V_0}\frac{A_i}{\rho L_i} \quad \mathrm{B}=\frac{\omega}{\sqrt{\Omega_1^2+\Omega_2^2}}, \quad i=1,2 \tag{12}$$

The transfer function then takes the form

$$H_v(s)=2k_0\frac{s^2+2s\left(\zeta_1\Omega_1+\zeta_2\Omega_2\right)+4\zeta_1\Omega_1\zeta_2\Omega_2}{s^3+2s^2\left(\zeta_1\Omega_1+\zeta_2\Omega_2\right)+s\left(4\zeta_1\Omega_1\zeta_2\Omega_2+\Omega_1^2+\Omega_2^2\right)+2\left(\zeta_1\Omega_2+\zeta_2\Omega_1\right)} \tag{13}$$

5. ACTUATOR GEOMETRY AND MATERIAL PROPERTIES

The following key actuator dimensions and material properties were used in the analysis and for the experimental, purpose-built single-path piston MR damper. In the dual-path piston geometry, each of the flow channels was configured to have the same area factor and hydraulic resistance as in the single-path piston (Tab. 1).

Table 1. Values used in the analysis and experiment

Parameter	Value
Fluid dynamic viscosity	35 cP
Bulk modulus	100 MPa
MR fluid density	2.35 g/cm^3
Area factor	1662.0 mm^2
Annulus thickness (flow gap)	1.0 mm
Annulus cross section area	118.2 mm^2
Annulus length	34.0 mm
Chamber #1 (#2) length (at mid-stroke)	34.0 mm

6. ANALYTICAL RESULTS

In this Section, the stroke-driven model is analyzed and compared to the detailed model developed in [1]. The multiple flow-path piston dynamics is briefly analyzed as well.

6.1. Single-path piston dynamics

The calculated results for the model (4) are illustrated in Figures 8–12 as Bode plots of the amplitude and phase angle against frequency. Again, the input force frequency was normalized with respect to the 'slug' natural frequency, Ω_F. On analyzing the results revealed in Figures 8–12, it can be noted the simplified model and the detailed model in [1] (revealed in Figs. 8 and 9) share the same first resonant frequency, Ω_F. To have a fair comparison of the results, the detailed force-driven model was made symmetric and had no gas chamber on the compression side of the piston. Comparing Figures 8–12, the authors noted that the frequency responses calculated by means of the detailed model and the transfer function of Eq. (4) match well up to the first resonant frequency. Model (4), which is driven by a prescribed piston velocity profile, ignores the (typically small) influence of the P&R mass on the frequency response within the frequency range from 0 to Ω_F.

6.2. Dual-path piston dynamics

A similar analysis was performed by the authors for the dual-path piston model (11). In the analysis, the flow paths were assumed identical in terms of the area factor and the hydraulic resistance. The hydraulic resistance of each of the flow paths in the dual-path piston was made equal to that of the single-path piston. Again, the data sets were scaled with respect of the 'slug' natural frequency of the single-gap piston, Ω_F. The results for the dual-path piston in Figures 13–15 reveal very good frequency-dependent characteristics in terms of both resonant frequency and the phase shift – both metrics are superior for the dual-path piston system. In the previous study [1] the authors concluded that the control over the phase shift is critical for the high-frequency behavior of the damper. In this respect, the dual-path piston reveals a far better behavior that the single-path damper.

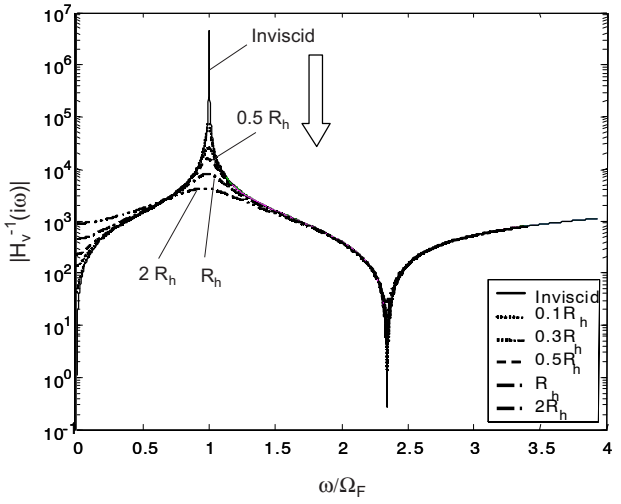

Fig. 8. H_v: *amplitude* variation with damping and input frequency

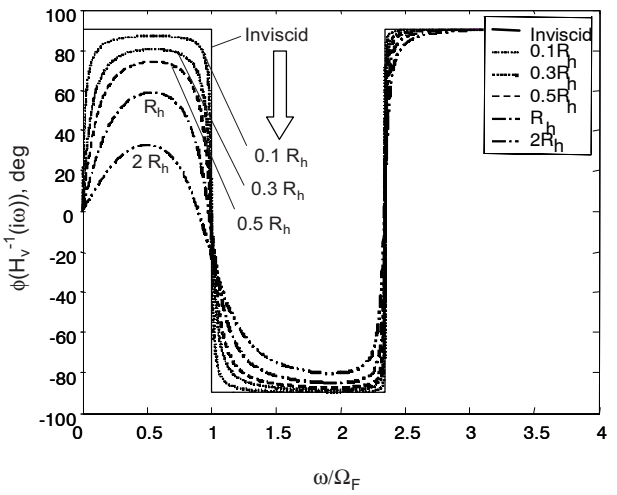

Fig. 9. H_v: *phase* variation with damping and input frequency

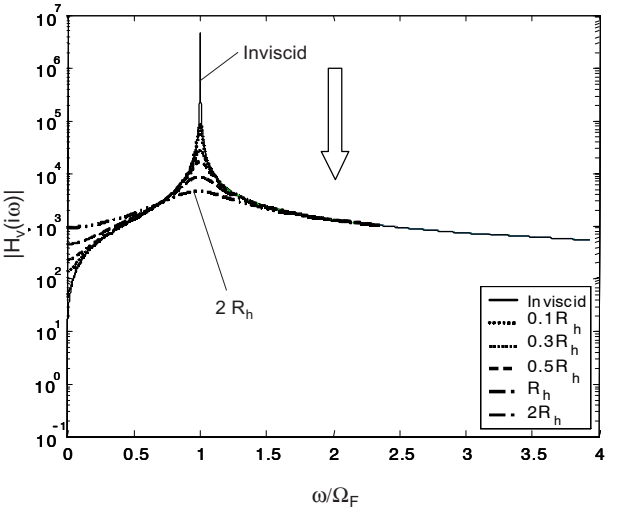

Fig. 10. H_v: *amplitude* variation with damping and input frequency

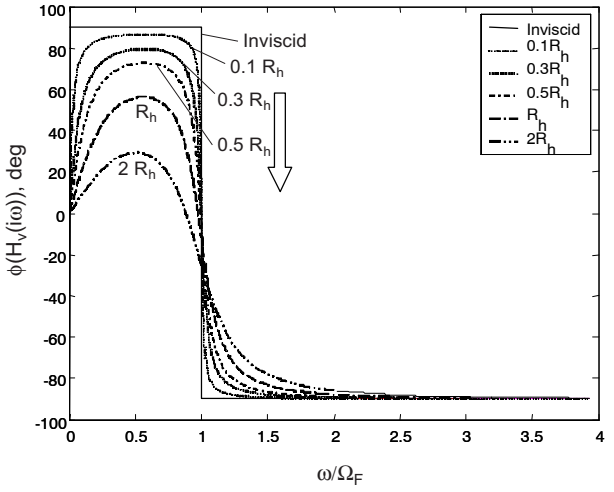

Fig. 11. H_v: *phase* variation with damping and input frequency

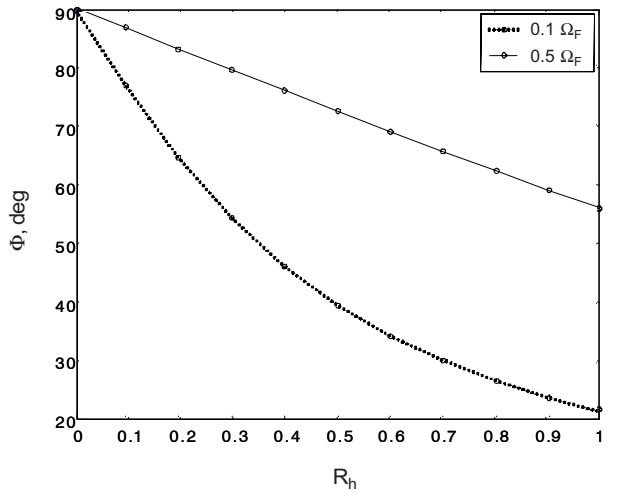

Fig. 12. H_v: The effect of the (laminar) flow resistance R_h on the phase angle

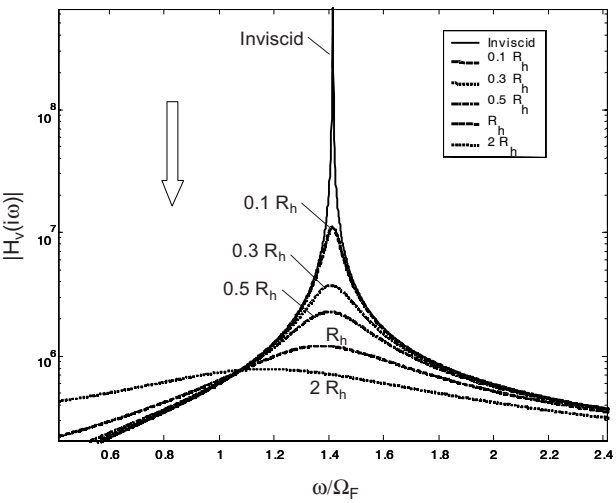

Fig. 13. H_v: *amplitude* variation with damping and input frequency; dual-path piston

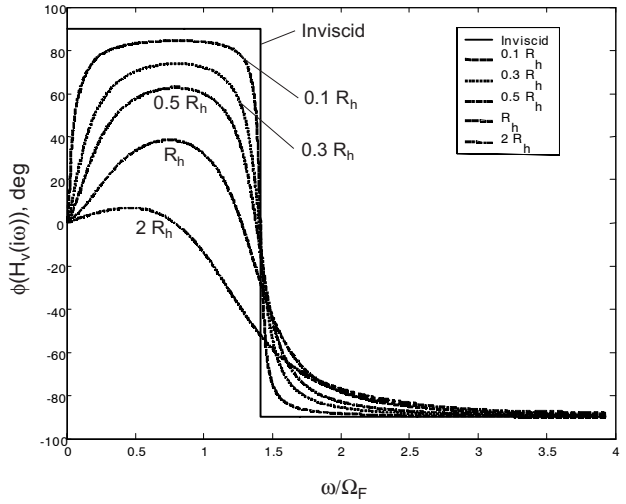

Fig. 14. H_v: *phase* variation with damping and input frequency; dual-path piston

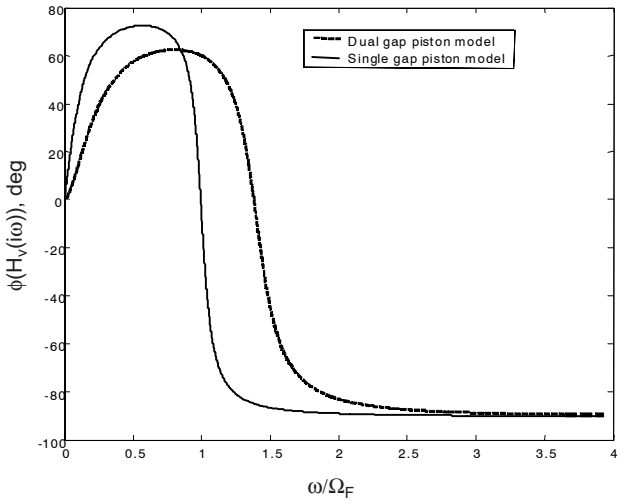

Fig. 15. *Phase shift*: comparison of the dual-path piston performance vs. single-path piston

7. SUMMARY AND CONCLUSIONS

In order to illustrate the validity of simplified dynamic models, the authors have performed an analysis of a stroke-driven monotube damper using linear state-space and frequency-domain techniques. Compared to the detailed model previously analyzed in [1], the results show that the performance of the simple model matches well the detailed model up to the first resonant frequency. In other words, the present simple model describes adequately the MR damper dynamics for frequencies up to the first natural frequency of the damper, Ω_F. The analysis was extended to piston configurations having two parallel flow channels and showed that the dual-path configuration provides superior performance as compared to the single-path in the sense that the first natural frequency is higher and the phase shift is less pronounced in the low frequency range.

Finally, the authors derived mechanical spring-mass-damper analogies for the single- and dual-path piston configurations.

References

[1] Alexandridis A.A., Goldasz J.P.: *High-frequency Dynamics of Magneto-Rheological Dampers.* [In:] Proceedings of the Ninth International Conference on New Actuators-ACTUATOR 2004, Bremen, Germany, 14–16 June, 2004

[2] Namuduri C., Alexandridis A.A., Madak J., Rule D.S.: *Magnetorheological Fluid Damper with Multiple Annular Flow Gaps.* US Patent 6,279,701, 2001